



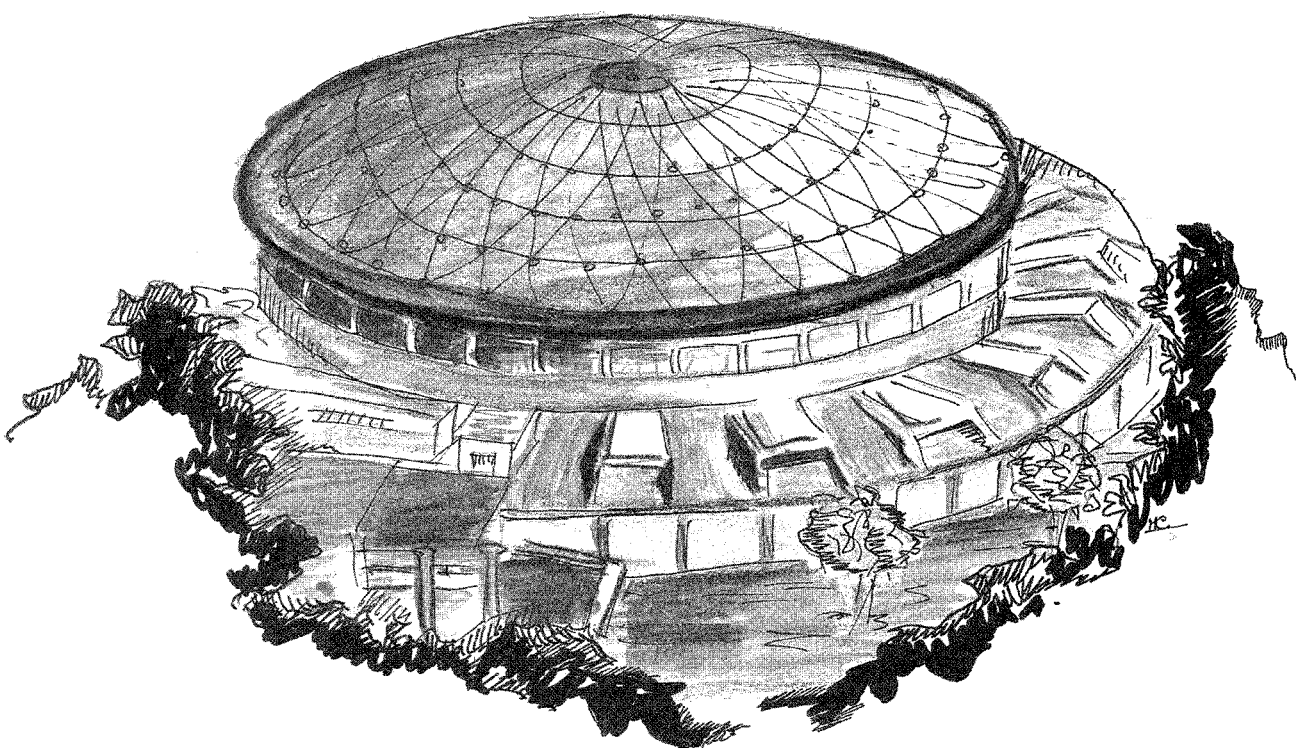
ISTITUTO NAZIONALE DI FISICA NUCLEARE - ISTITUTO NAZIONALE DI FISICA NUCLEARE

Laboratori Nazionali di Frascati

LNF-89/086(R)
11 Dicembre 1989

C.Biscari:

LISA CAPTURE SECTION: SIMULATION OF PARTICLE DYNAMICS



Servizio Documentazione
dei Laboratori Nazionali di Frascati
P.O. Box, 13 - 00044 Frascati (Italy)

LNF-89/086(R)
11 Dicembre 1989

LISA CAPTURE SECTION: SIMULATION OF PARTICLE DYNAMICS

C.Biscari

INFN - Laboratori Nazionali di Frascati, P.O. Box 13, 00044 Frascati (Italy)

Introduction

The beam of LISA, produced at 100 keV kinetic energy, is accelerated by a capture section to 1.1 MeV before the injection into the SC Linac. The capture section has been constructed in Swierk laboratory and is presently under test in ours. It is a 1 MeV standing wave accelerator, 2.5 GHz. Its characteristics are described in references [1-2].

The beam transverse focalization is ensured by a solenoidal winding around the section, which produces a more intense magnetic field at the low energy part of the accelerator. The longitudinal magnetic field has been measured^[2] for different values of the current in the windings.

Up to now constant magnetic field had been assumed in particle dynamics simulation through the section^[3]. The actual configuration of the magnetic field will now be used. A fitting procedure has been followed in order to have an analytical expression of the magnetic field to be used in tracking codes. Particle dynamic simulation along the section has been carried out for the nominal current of 2 mA.

Analytical treatment of the measured magnetic field

The longitudinal axial magnetic field B_z produced by the solenoid has been measured^[2] for three values of the current in the solenoid ($I = 50, 60, 70$ A). The measurements are reported in fig. 1.

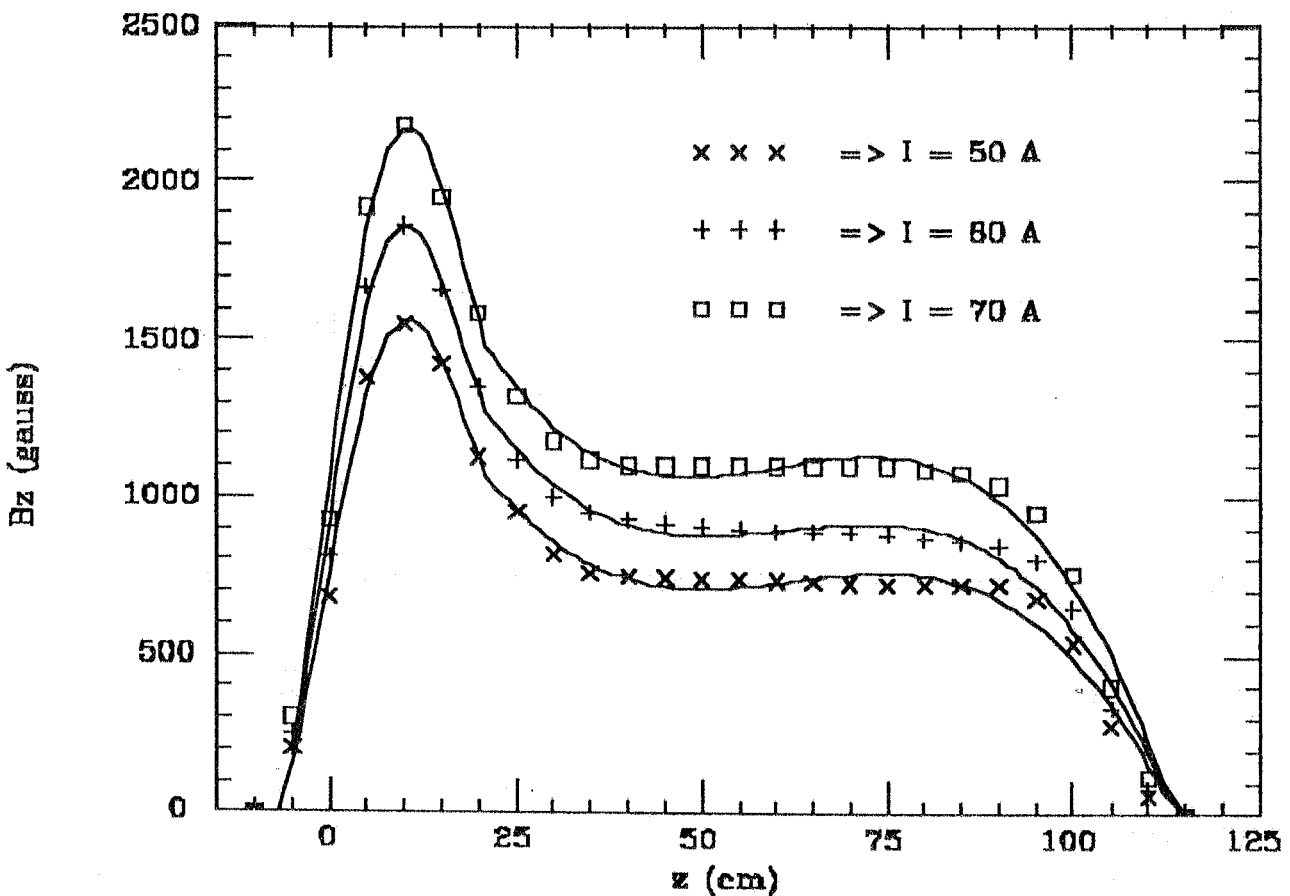


Fig.1 - Measured longitudinal magnetic field produced by the solenoid of the capture section with three different values of the current in the windings. The full curves represent the polynomial fit of the measures.

The tracking code presently in use at Frascati, PARMELA^[4], does not work with numerical values of the fields, while it is possible to introduce in the program an analytical expression of a specified field and solve the correspondent motion equations. A polynomial fit of the magnetic field measured values has been done for each one of the three currents. The points represented in fig.1 are easier to fit with two different polynomials, so the profile has been divided into two zones:

$$\begin{aligned}
 B_z(I_i) &= \sum_{n=1}^5 a_{i1n} z^{n-1} & z_I < z \leq z_C \\
 B_z(I_i) &= \sum_{n=1}^4 a_{i2n} z^{n-1} & z_C < z < z_F
 \end{aligned} \tag{1}$$

where $z_I = -10$ cm, $z_F = 115$ cm, $z_C = 20$ cm (the origin of the z -axis corresponds to the beginning of the accelerating field inside the accelerator, as in fig.1); $I_i = 50, 60, 70$ A respectively for $i = 1, 2, 3$. The fit has been carried out utilizing the least squares method of the LSQ subroutine of the CERN library^[5], with the first 7 points for the first fit and the last 20 points for the second one. The set of coefficients a_{ikn} ($i=1, 2, 3$; $k=1 \text{ or } n=1, \dots, 5$; $k=2 \text{ or } n=1, \dots, 4$) is given in Table I for B_z measured in gauss and z in cm. In fig.1 the curves (1) are represented by the full lines.

Table I - Coefficients a_{ikn}

n	1	2	3	4	5
a_{11n}	760.1948	129.7965	-1.309091	-0.5236363	1.5515151E-02
a_{21n}	923.3117	157.7078	-1.904545	-0.6551515	2.0424243E-02
a_{31n}	1062.792	180.5996	-1.896970	-0.7321212	2.1939393E-02
a_{12n}	2120.954	-72.83677	1.219662	-6.5402850E-03	
a_{22n}	2430.217	-80.28806	1.351331	-7.3285000E-03	
a_{32n}	2803.245	-92.49374	1.594805	-8.7847915E-03	

The expressions (1) are not yet utilizable for our purpose; in fact they are valid only for the three values of I considered in the measurement, while we are interested in an expression of the magnetic field with a general dependence on the current I : a linear fit of each group of three coefficients (a_{ikn} , $i=1,2,3$) has been done so that defining

$$A_{kn}(I) = b_{kn} + c_{kn} \quad (2)$$

B_z can be written as

$$B_z(I) = \sum_{n=1}^5 A_{1n}(I) z^{n-1} \quad z_I < z \leq z_C$$

$$B_z(I) = \sum_{n=1}^4 A_{2n}(I) z^{n-1} \quad z_C < z < z_F \quad (3)$$

The coefficients b_{kn} and c_{kn} are listed in Table II. The resulting curves for values of I between 40 and 70A are represented in fig. 2 as full lines together with the measured values for comparison. Of course the expressions (3) are not

valid for vanishing I , but only for realistic values of the current, as those represented in the figure.

Table II - Coefficients b_{kn} and c_{kn}

n	1	2	3	4	5
b_{1n}	7.641199	3.625386	6.0100794E-02	-1.1514735E-02	2.0208023E-05
c_{1n}	15.12986	2.540154	-2.9393936E-02	-1.0424249E-02	3.2121202E-04
b_{2n}	404.5974	-22.90200	0.2631677	-8.1768021E-04	
c_{2n}	34.11458	-0.982848	1.8757189E-02	-1.1222520E-04	

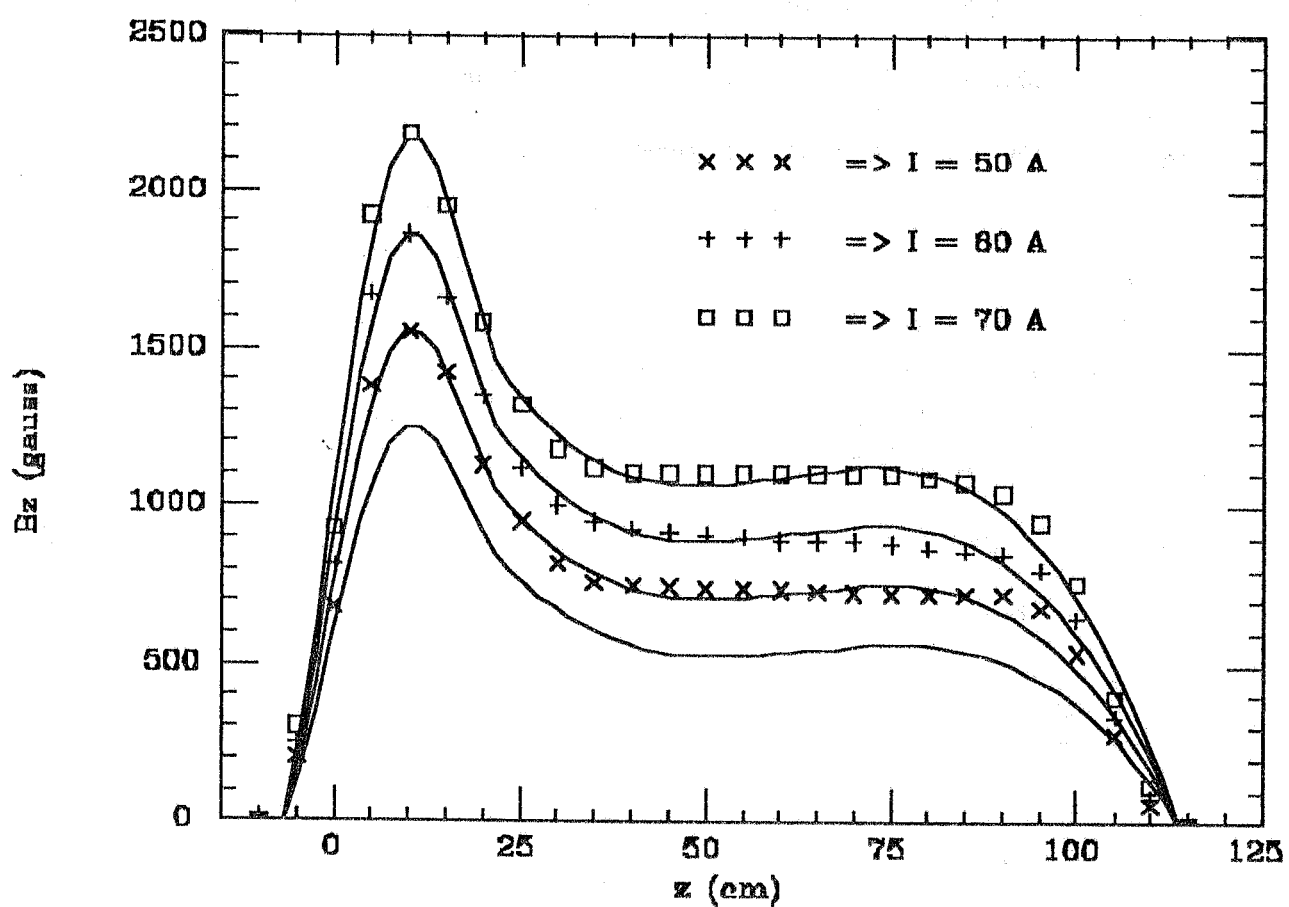


Fig. 2 - General expression of the longitudinal magnetic field along the section parametrized with the current I in the windings. The measures are reported for comparison.

Particle motion along the section

The accelerator cavity is divided into 23 cells, $\beta\lambda/2$ long; their dimensions are listed in Table III. The average accelerating electric field is of the order of 1 MV/m.

In PARMELA the effect of the rf field on the particle dynamics is simulated by a kick at the beginning of each integration step, drifting then the particle coordinates if in absence of external magnetic field. If an external magnetic field is also present in the structure the particle coordinates are integrated with the law of propagation in the magnetic field.

Table III - Cell lengths in the capture section

Cell number	Length (cm)
1	3.5376
2	3.9072
3	4.1550
4	4.3678
5	4.5504
6	4.7074
7	4.8426
8	4.9594
9	5.0608
10	5.1492
11	5.2262
12	5.2938
13	5.3534
14	5.4062
15	5.4528
16	5.4946
17	5.5318
18	5.5652
19	5.5952
20	5.6222
21	5.6466
22	5.6690
23	5.6844

The magnetic field configuration described above has been introduced in the program^[4]. Defining

$$M = B_z/B\rho$$

$$K = \partial M / \partial z$$

the equations of motion can then be written as

$$x'' = y'M - yK/2 \quad (4)$$

$$y'' = -x'M + xK/2$$

and the particle coordinates are obtained integrating (4) with a RungeKutta method.

The effect of the solenoid on the beam at the section entrance is defocalizing because of the high positive field gradient, and the defocalization begins even before the acceleration. It is then necessary that the beam should have a negative divergence when it arrives to the accelerating field to avoid an increase of the transverse envelope which could make particles hit the cavity walls; to this purpose an additional magnetic lens, not foreseen before^[6], will be positioned before the capture section as near as possible to it. It will be fed by the same power supply as the main solenoid.

Particle motion simulation has been carried out for the nominal average current of 2mA, corresponding to a charge of 40pC per bunch. The beam has been followed from the gun to the end of the section. The necessary current in the solenoid is 51 A. The longitudinal magnetic field of the lens before the capture section has been simulated by a gaussian distribution with $\sigma = 5\text{cm}$; the necessary peak value is $B_0 = 200$ gauss.

The transverse envelopes, transverse emittances, and length of the bunch along the whole injection sistem are given in figs.3/5. The emittance bumps are in correspondence of the magnetic field produced by the focalizing lenses and do not mean an effective increase of the emittance; they appear because in the computation of the emittance value the transverse momenta are rotated by the longitudinal component of the magnetic field. The beam transverse parameters at the gun are taken from previous work^[3]: $\epsilon = 1 \times 10^{-5} \text{ m rad}$, $\sigma = 0.5 \text{ mm}$. The characteristics of the bunch at the input and output of the section are given in Table IV.

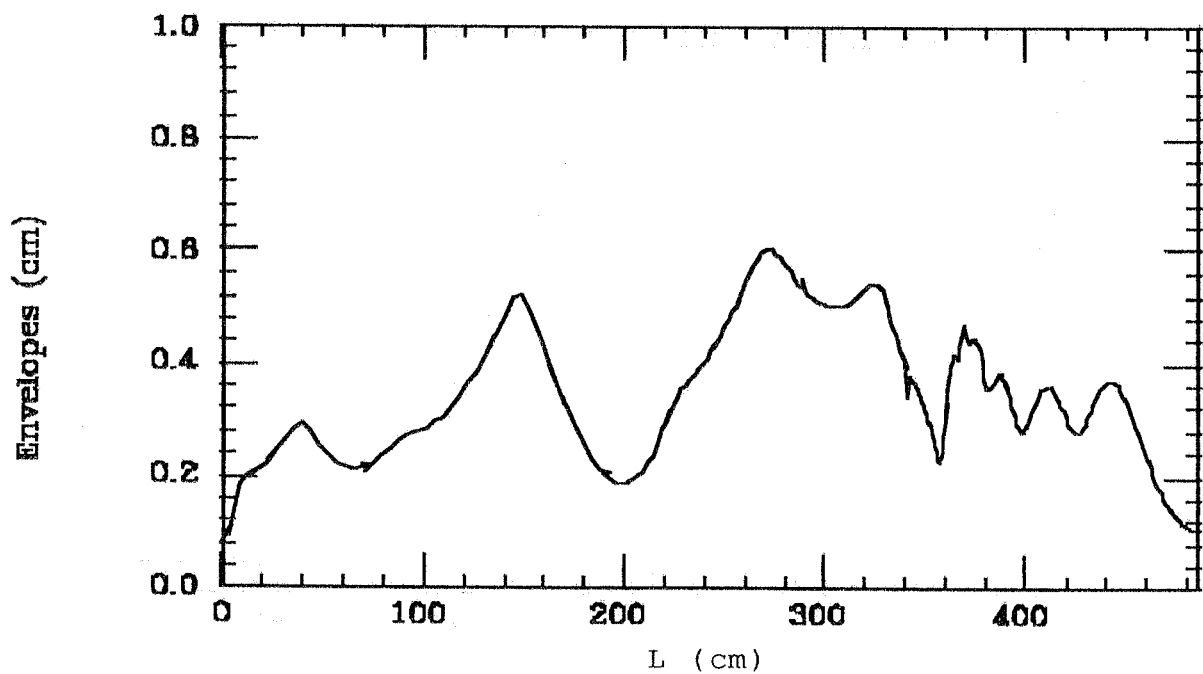


Fig.3 - Transverse envelope along the whole injection system, from the gun to the exit of the capture section

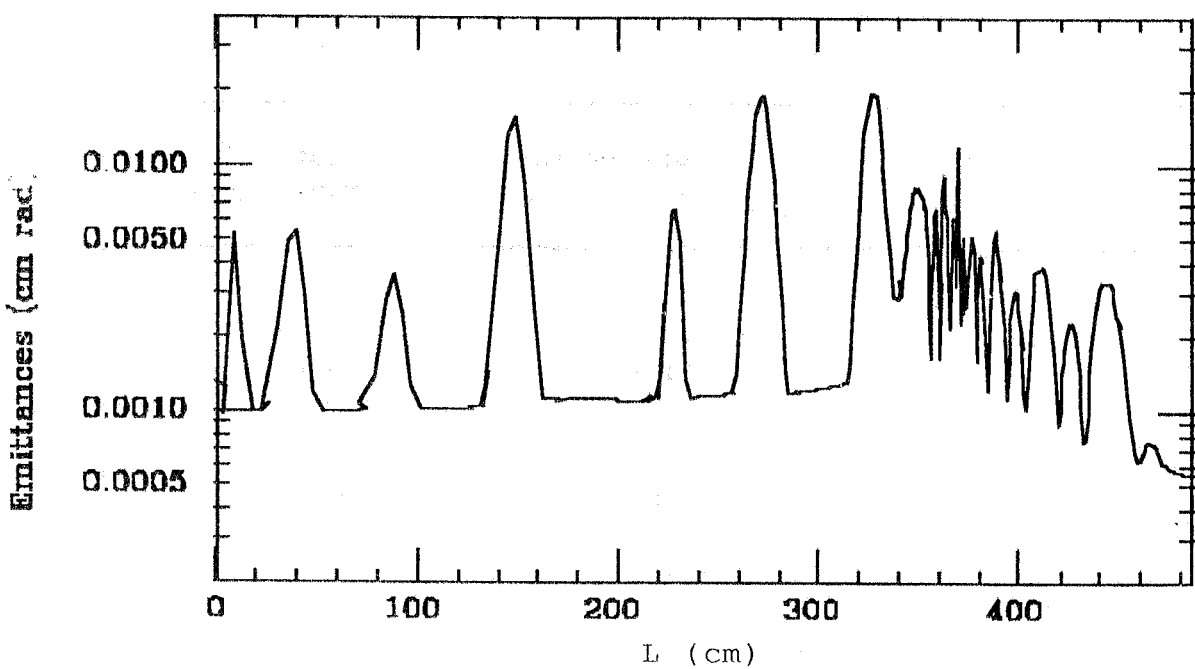


Fig.4 - Transverse emittance along the whole injection system from the gun to the exit of the capture section.

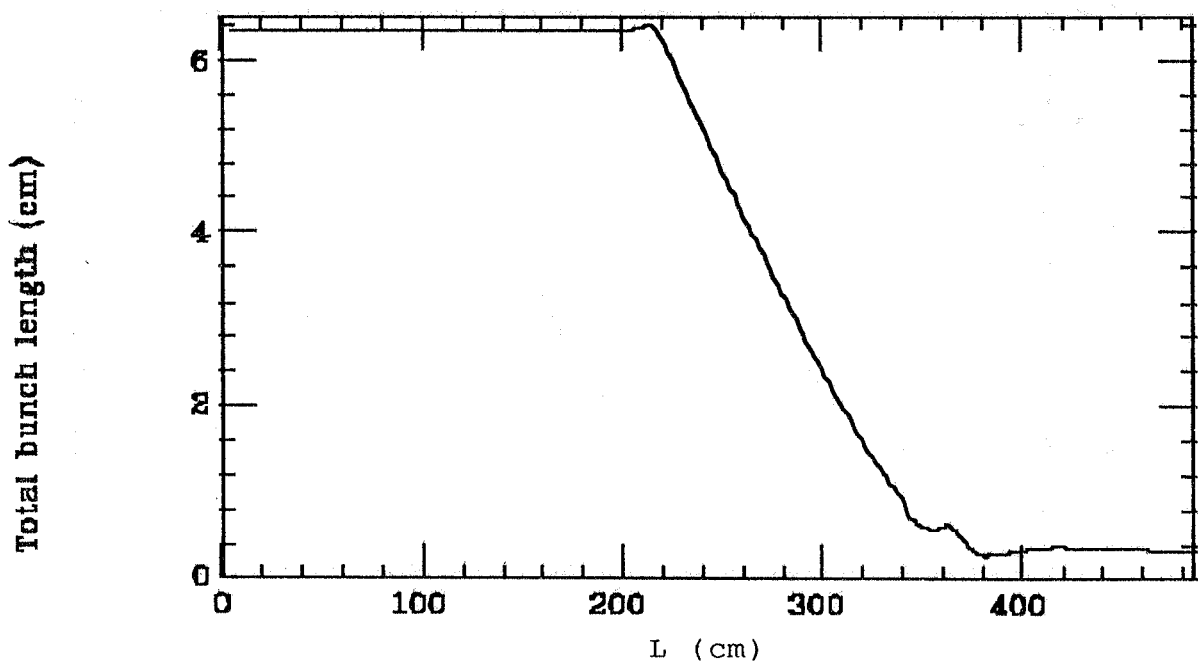


Fig.5 - Bunch length along the whole injection system. Up to the chopper ($L \approx 200$ cm) the beam is continuous. From the prebuncher to the capture section the bunch length shortens by a factor ~ 13 and is further diminished along the section.

Table IV - Bunch parameters at the capture section ends

Parameter	Input of the capture section	Output of the capture section
σ (mm)	3.1	1.2
ϵ (m rad)	1.8×10^{-5}	5.6×10^{-6}
ϵ_n (m rad)	1.2×10^{-5}	1.8×10^{-5}
β (m)		0.24
α		0.66
E (MeV)	0.098	1.17
$\Delta E/E$ (%)	± 4.5	± 1.5
$\Delta p/p$ (%)	± 2.4	± 1.1
Bunch length (85%): (mm)	7.	2.
$\Delta\phi$ ($^\circ$ @ 2500 MHz)	40.	6.
I_{av} (mA)	2.	2.
I_p (A)	< 1	5.4

The right magnetic field must be used to minimize the emittance at the exit of the section. In fact the particle trajectory inside the capture section follows in the transverse plane the helicoidal path imposed by the solenoid magnetic field and the rf field. If the number of cycles inside the accelerating field is not an integer the particle will be transversally defocalized when it exits the section. In fig. 6 the trajectories of a test particle in the (x,y) plane are plotted for three values of the magnetic field; the trajectories are followed inside the capture section and in the 10 cm drift after the section. The value of the magnetic field which minimizes the emittance corresponds to $I=50.95\text{A}$: the trajectory, after following different circles, is focalized towards the axis. For $I=49\text{A}$ the last circle is not closed and the particle exits the accelerator with a big divergence. For $I=53\text{A}$ the last circle has a very small curvature radius and the particle is given a strong defocalizing kick. The effect on the transverse phase plane can be viewed also in fig. 7: the non-optimized magnetic field produces an almost hollow distribution which, together with the dilution in the phase plane, is responsible of a big increase in the emittance value; to be noticed that this increase occurs just at the exit of the section: along the accelerator the three solutions are similar. The stability of the optimum solution is shown in fig. 8, where the beam emittance at the exit of the capture section is plotted versus the current in the solenoid; the emittance value oscillates and it will not be difficult to find the right value of I if an emittance measurement device is placed after the section.

The longitudinal phase space is affected by the space charge force, especially at the lower energies, and so the prebuncher cannot be used at its maximum power to contain the emittance blowup produced by the current density increase in the 100 keV microbunch^[6]; the bunch, when it enters the section, is 40° rf long (@2500 MHz, i.e. 7 mm). All the beam is accepted in the section and at its output 85% of the initial current is contained in $\sim 6^\circ$, i.e. 2 mm, while the remaining 15% is distributed in long tails. The peak current is 5.4 A. The evolution of the longitudinal phase space along the section is plotted in figs. 9 and 10. In fig. 11 the phase distribution of 90% of the total beam is given.

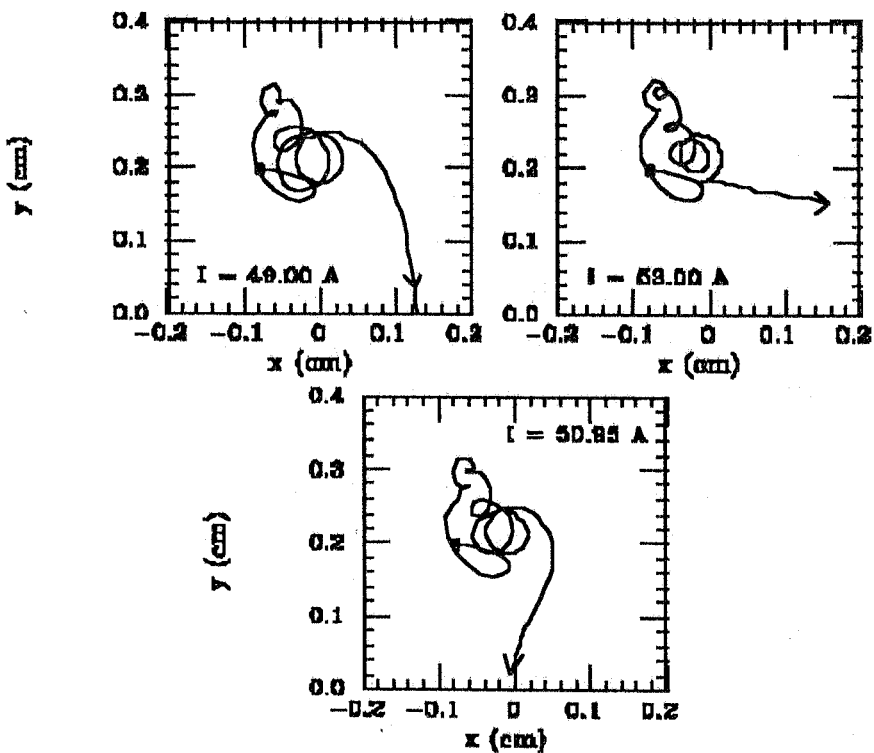


Fig. 6 - Trajectories in the (x,y) plane of a test particle inside the capture section with three different values of the current in the solenoid. The circle indicates the starting point.

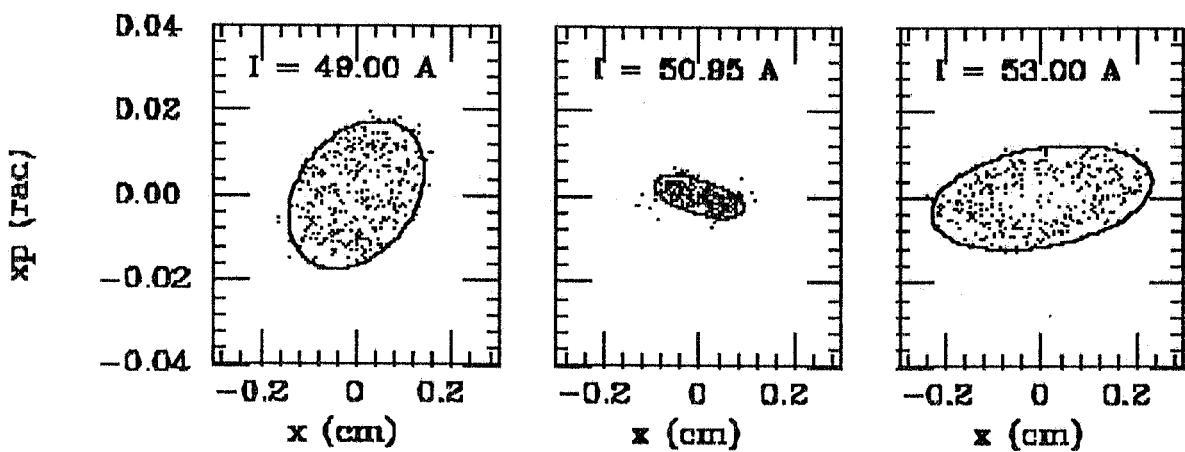


Fig. 7 - Horizontal phase space at the exit of the capture section for three different values of the current in the solenoid

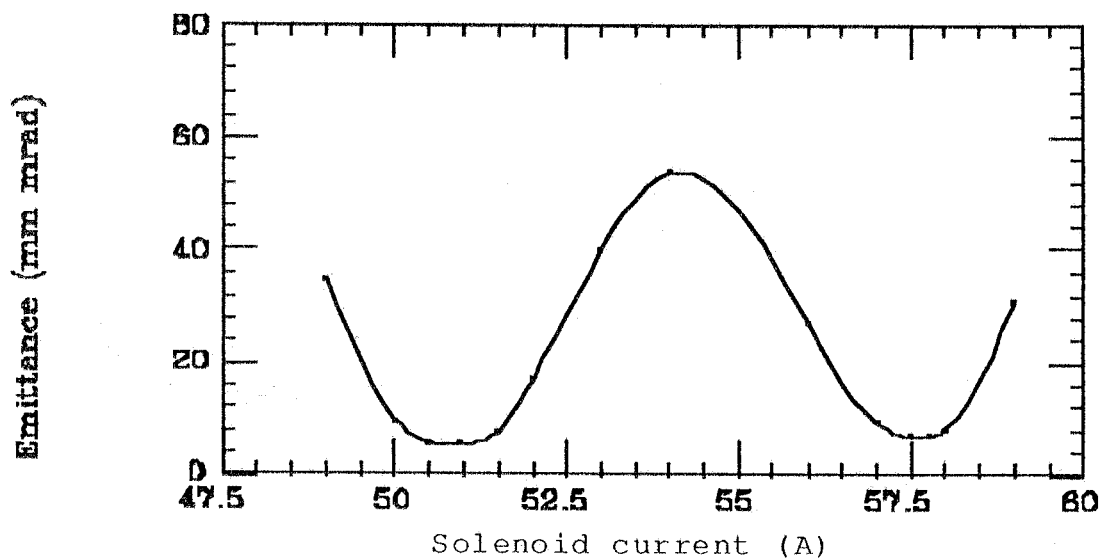


Fig.8 - Beam emittance at the exit of the capture section versus the current I in the solenoid

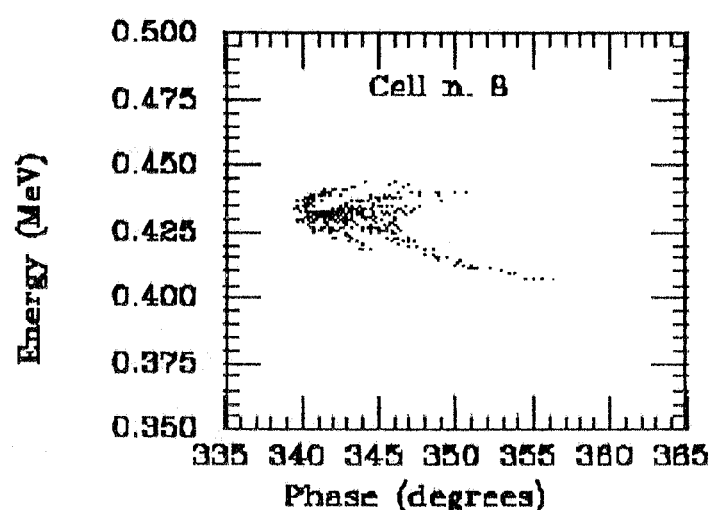
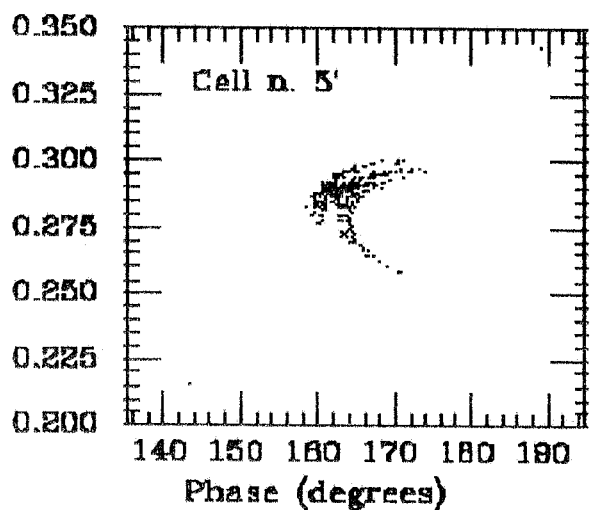
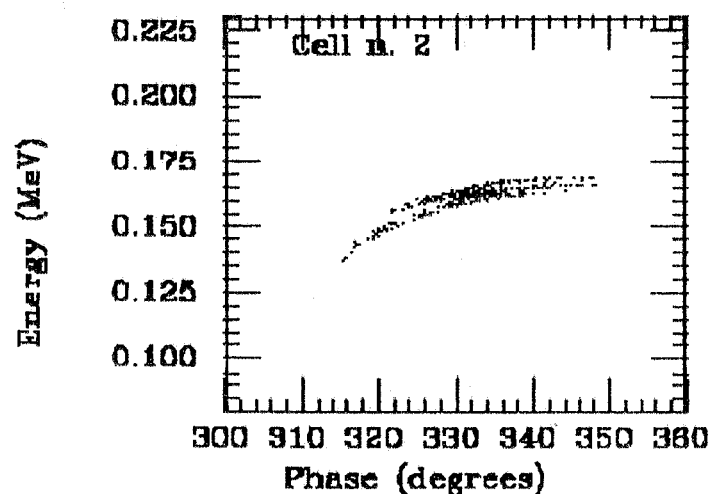
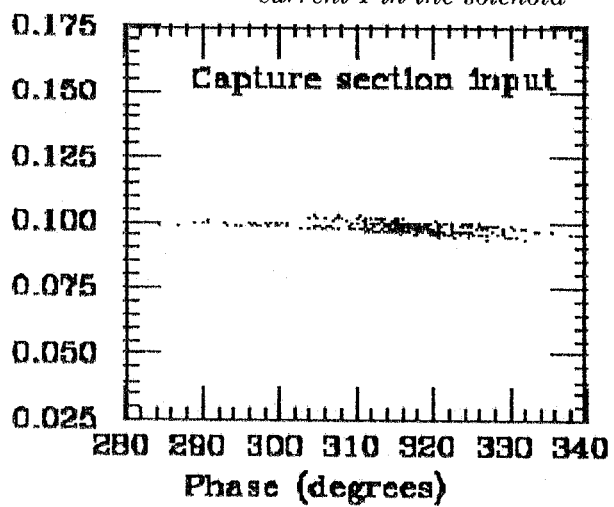


Fig.9 - Longitudinal phase space along the low energy part of the capture section

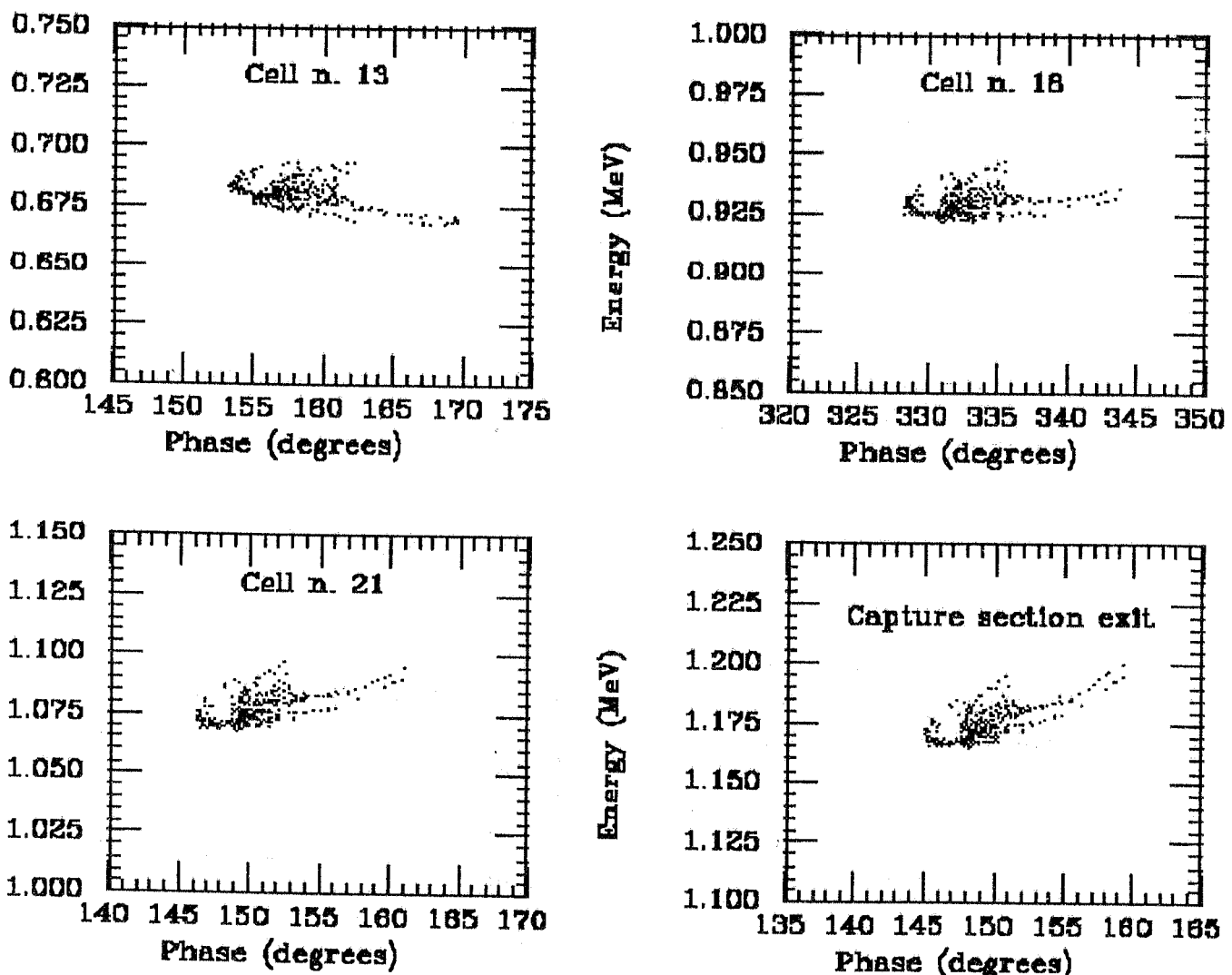


Fig.10 - Longitudinal phase space along the high energy part of the capture section

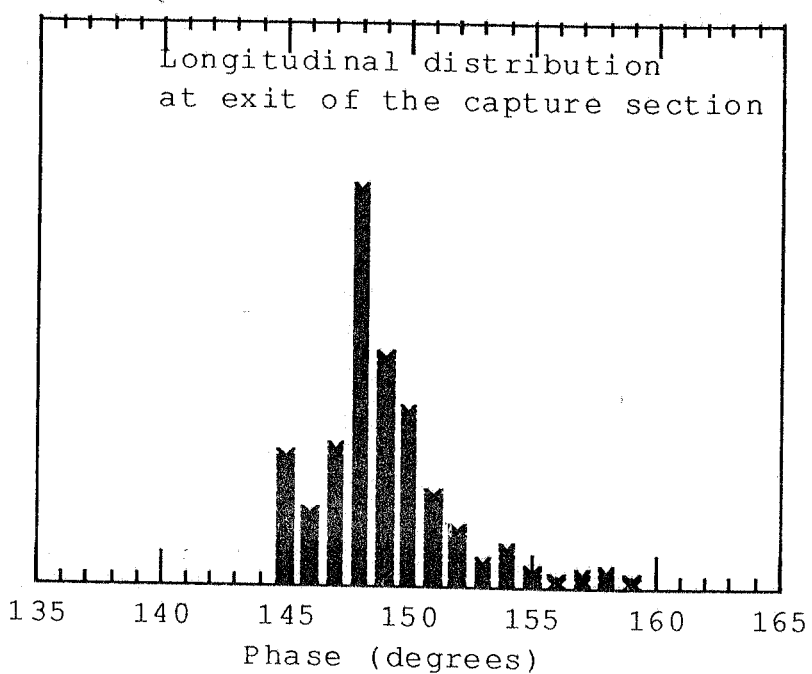


Fig. 11 - Longitudinal bunch distribution at the exit of the capture section

References

- [1] - J.Bigolas et al. - "Technical Project for Design and Construction of 1MeV S.W. accelerating structure in injection system to superconducting electron accelerator LISA at INFN - Frascati" - Swierk, 1988
- [2] - J.Bigolas et al. - "Assembling and acceptance test report of 1.1MeV Capture Accelerating Structure for LISA Accelerator at Frascati" - Swierk, June 1989
- [3] - A.Aragona, C.Biscari, R.Boni, S.Kulinski, B.Spataro, F.Tazzioli e M.Vescovi - "The injector for LISA" - Proceedings of the Linear Accelerator conference 1988 - Williamsburg USA - October 1988
- [4] - C.Biscari - "PARMELA at LNF" - in preparation.
- [5] - E.Keil - "Least Squares Polynomial Fit" - KERNLIB - E208 (1969) - Cern Program Library
- [6] - C.Biscari - "Particle dynamics in the 100 keV injector of LISA" - LNF - 88/3 (NT) - (1988)